

Microchannel Cooling Systems Using Dielectric Fluids

**Dorin LELEA, Ioan LAZA and
Liviu MIHON**

University Politehnica Timisoara, Faculty
of Mechanical Engineering Department of
Thermal Machines and Transportation
B-dul Mihai Viteazu nr. 1, 300222 Timisoara,
Romania

ldorin@mec.upt.ro

Keywords

*Dielectric fluid
Impingement jet
Microtube heat sink
Numerical modeling
Single-phase*

Ključne riječi

*Dielektrični fluid
Naletni mlaz
Izmjenjivač topline s mikrocijevima
Numeričko modeliranje
Jednofazni*

Received (primljeno): 2010-12-01

Accepted (prihvaćeno): 2011-02-07

1. Introduction

The thermal management of the electronic devices and power sources became the challenging issue in the last decade because of both, miniaturization and heat transfer rate increasing. The various cooling solutions have been proposed using both the single and two-phase heat transfer. Since this paper deals with the single phase heat transfer of water, only these cooling solutions will be considered.

The advantage of the single-phase microchannel heat sink, is based on an increase the heat transfer coefficient as the hydraulic diameter is decreasing. Also the channel walls are acting as the fins that increase the heat transfer area. For the case of the microchannel heat sinks, the investigations are made for single layer arrangement [1-6] and double layer arrangement [7-8]. The research has been made experimentally and numerically although the analytical solution based on a porous model has been

Original scientific paper

This paper presents the numerical investigation of the microtube heat sink with impingement jet feeding and HFE-7600 dielectric fluid. The inlet channel covers only a quarter of the tube perimeter so the swirl flow is settled in the tubes and the heat transfer between the liquid flow and silicon substrate is improved. The variable physical properties are used as the working fluid and turbulent flow regime is considered. The proposed microtube heat sink with impingement jet feeding was compared with a classic microtube heat sink with paralel inlet and outlet cross sections in terms of temperature variation along the heated surface and temperature difference. The influence of the temperature dependent physical properties on the fluid flow and heat transfer is analyzed and compared with results obtained for water as the working fluid.

Mikrokanalni rashladni sustavi koristeći dielektrične fluide

Izvorno znanstveni članak

Ovaj rad predstavlja numeričku analizu strujanja i prijenosa topline dielektričnog fluida HFE-7600 u mikrocijevnom izmjenjivaču topline s nastrojavanjem naletnim mlazom. Kako poprečni presjek ulaznog kanala pokriva samo četvrtinu cijevi, uspostavlja se vrtložno strujanje unutar mikrokanala i samim tim dolazi do poboljšanja toplinskog učina aparata. Uzete su u obzir toplinske karakteristike fluida u zavisnosti od temperature i turbulentni režim strujanja. Rezultati predloženog modela upoređivani su s toplinskim učinkom klasičnog mikro-cijevnog izmjenjivača topline s paralelnim ulaznim i izlaznim poprečnim presjecima po promjeni temperature kontaktne površine između izmjenjivaca topline i izvora topline. Također su upoređivani rezultati sa slučajem u kojem je voda radni fluid i analiziran je utjecaj temperaturno zavisnih karakteristika radnog fluida.

announced [9]. The fractal branching microchannel heat sink was investigated in [10]. Also, the viscous dissipation effect and the slip flow regime were considered for rectangular microchannel heat sinks [11-12]. In addition, the review chapters on micro-heat sinks might be found in [13-14].

Contrary to the microchannel heat sink, Soliman et al [15] presented the results for the numerical modeling made on microtube heat sink. The constant property laminar heat transfer of the water through the microtubes is considered. It was found that proposed heat sink have higher thermal resistance and requires lower pumping power compared to the microchannel heat sink for the same Re and hydraulic diameter. On the other hand, based on the unit pumping power, the microtube heat sink can dissipate slightly larger heat rate than the microchannel heat sink.

Besides, Ryu et al [16] have presented the numerical analysis of the manifold microchannel heat sink. It is

Symbols / Oznake	
B	- micro-heat sink width, m - širina mikro-hladnjaka
b_{ch}	- inlet channel width, m - širina ulaznog kanala
c_p	- specific heat, J/kg K - specifična toplina
D_i	- inner diameter, m - unutarnji promjer
h_{ch}	- inlet channel height, m - visina ulaznog kanala
H	- micro-heat sink height, m - visina mikro-hladnjaka
k	- thermal conductivity, W/m K - toplinska vodljivost
L_{ch}	- inlet channel length, m - duljina ulaznog kanala
L	- micro-heat sink length - duljina mikro-hladnjaka
M	- mass flow rate, kg/s - maseni protok
N	- number of the channels - broj kanala
Δp	- pressure drop, Pa - pad tlaka
q	- heat flux, W/cm ² - toplinski tok
R	- thermal resistance, cm K/W - toplinski otpor
Re	- Reynolds number - Reynoldsov broj
T	- temperature, K - temperatura
T_{max}	- peak temperature - vršna temperatura
ΔT	- temperature difference - temperaturna razlika
u, v, w	- velocity, m/s - brzina
w_m	- module width, m - širina modula
x, y, z	- Coordinate, m - koordinatne osi
μ	- dynamic viscosity, Pa s - dinamička viskoznost
ρ	- density, kg/m ³ - gustoća
Π	- pumping power, W - snaga crpke
Indices / Indeksi	
in	- inlet - ulaz
out	- outlet - izlaz
f	- fluid - tekućina
s	- solid - krutina

concluded that this heat sink has better performances than the classical microchannel heat sink, lower thermal resistance and more uniform temperature distribution for the same pumping power. The optimization of the heat sink geometric parameters is done to obtain the best heat transfer characteristics.

The numerical analysis of the partially heated microchannel heat sink was reported by Lelea [17] while the performance evaluation of the nanofluid cooled microchannel heat sink was presented by Lelea [18]. Sung and Mudawar [19] analyzed the hybrid jet impingement microchannel heat sink in turbulent heat transfer and fluid flow. It was shown that the vorticity has the large influence on a zone outside the impingement jet. The stronger attachment of the fluid flow to the heated surface for higher Re is observed. It was also proposed the improved design of the heat sink based on the optimized analysis that lowers the temperature distribution of the heated surface.

Following this review of the cooling solutions used for electronic and high power devices, the microtube heat sink with impingement jet is analyzed. The novel concept of the microchannel tangential cooling was introduced by Lelea [20,21]. In this case, instead of water, the dielectric fluid HFE-7600 is used and turbulent fluid flow condition is imposed.

2. Problem description and numerical details

The microtube heat sink assembly proposed for numerical analysis is presented in the Figure 1. It might be observed that feeding of the microtube heat sink is realized through the gaps on the top surface of the heat sink. The cross section of the microtube with the inlet channel is presented in the Figure 2. It can be noticed that the microtube is thermally and hydrodynamically

symmetrical with respect to the boundary positioned at the half-length of the microtube. So, only the left part of the microtube is analyzed. The set of the Navier-Stokes equations can be used, as follows:

The conservation of mass

$$\frac{\partial(\rho \cdot u_i)}{\partial x_i} = 0 \tag{1}$$

The conservation of momentum

$$\frac{\partial(u_i \cdot \rho \cdot u_j)}{\partial x_i} = -\frac{\partial p}{\partial x_i} + \frac{\partial}{\partial x_i} \left((\mu_f + \mu_t) \frac{\partial u_j}{\partial x_i} \right) \tag{2}$$

The conservation of energy

$$\frac{\partial(\rho \cdot c_p \cdot u_i \cdot T)}{\partial x_i} = \frac{\partial}{\partial x_i} \left((k_f + \frac{c_p \mu_t}{Pr_t}) \frac{\partial T}{\partial x_i} \right) \tag{3}$$

In addition for turbulent fluid flow the standard *k-ε* model is used:

The turbulence kinetic energy, *k*, and its rate of dissipation *ε* are obtained from the following transport equations:

$$\frac{\partial}{\partial t}(\rho k) + \frac{\partial}{\partial x_i}(\rho k u_i) = \frac{\partial}{\partial x_j} \left[\left(\mu + \frac{\mu_t}{\sigma_k} \right) \frac{\partial k}{\partial x_j} \right] + G_k + G_b - \rho \epsilon - Y_M + S_k \tag{4}$$

and

$$\frac{\partial}{\partial t}(\rho \epsilon) + \frac{\partial}{\partial x_i}(\rho \epsilon u_i) = \frac{\partial}{\partial x_j} \left[\left(\mu + \frac{\mu_t}{\sigma_\epsilon} \right) \frac{\partial \epsilon}{\partial x_j} \right] + C_{1\epsilon} \frac{\epsilon}{k} (G_k + C_{3\epsilon} G_b) - C_{2\epsilon} \rho \frac{\epsilon^2}{k} + S_\epsilon \tag{5}$$

In these equations, G_k represents the generation of turbulence kinetic energy due to the mean velocity gradients, calculated as described in Section, G_b is the generation of turbulence kinetic energy due to buoyancy, Y_M represents the contribution of the fluctuating dilatation in compressible turbulence to the overall dissipation rate, $C_{1\epsilon}$, $C_{2\epsilon}$, and $C_{3\epsilon}$ are constants, σ_k and σ_ϵ are the turbulent Prandtl numbers for *k* and *ε*, respectively, S_k and S_ϵ are user-defined source terms. The turbulent viscosity μ_t is computed as follows:

$$\mu_t = \rho C_\mu \frac{k^2}{\epsilon} \tag{6}$$

The model constants $C_{1\epsilon}$, $C_{2\epsilon}$, C_μ , σ_k and σ_ϵ have the following values:

$$C_{1\epsilon} = 1.44, C_{2\epsilon} = 1.92, C_\mu = 0.09, \sigma_k = 1.0, \sigma_\epsilon = 1.3, Pr_t = 0.85.$$

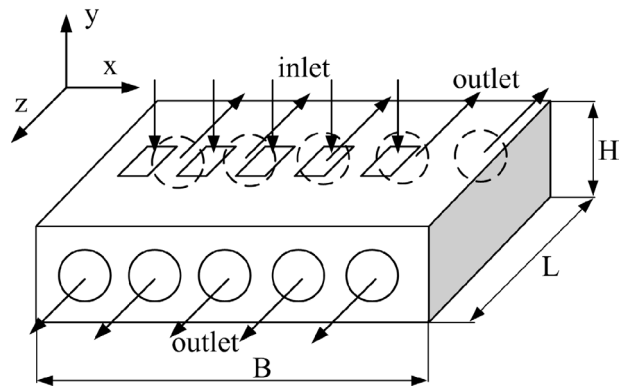


Figure 1. Microtube heat sink assembly with a tangential impingement jet

Slika 1. Mikrocijevni izmjenjivač topline s tangencijalnim naletnim mlazom

For the micro-tube heat sink presented in this paper, the following boundary conditions are settled:

- The fluid flow is stationary, incompressible and turbulent;
- The fluid properties of the HFE-7600 were considered as temperature dependent with following equations [22]:

Dynamic viscosity:

$$\mu(t) = (1587.5 - 1.755 \cdot t) \cdot 10^{-6} \cdot e^{\frac{464.403382}{t+133} - 2.881482}$$

Density:

$$\rho(t) = 1587.5 - 1.755 \cdot t.$$

Thermal conductivity:

$$k(t) = 0.078 - 0.0003 \cdot t.$$

Specific heat:

$$c_p(t) = 3.1631 \cdot t + 1240.2.$$

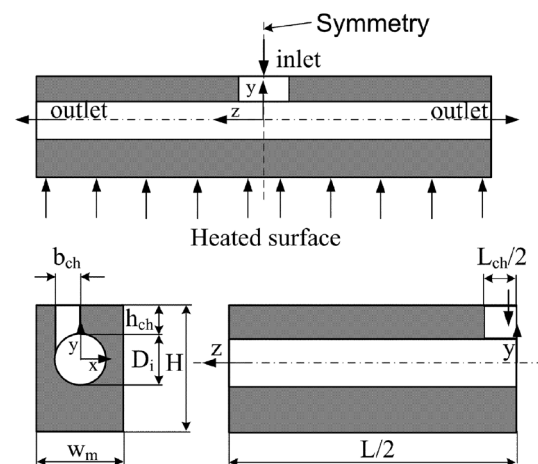


Figure 2. Geometry of a single microtube

Slika 2. Geometrija jedne mikrocijevi

- The uniform velocity field and the constant temperature are imposed at the channel inlet, while at the outlet the partial derivatives of the velocity and temperature in the stream-wise direction are vanishing;
- The conjugate heat transfer between the solid and fluid flow is considered and the no-slip velocity conditions at the solid-fluid interface;

The conjugate heat transfer procedure, implies the continuity of the temperature and heat flux at the solid – liquid interface defined as,

$$x = R_i : T_s|_{R^+} = T_f|_{R^-}$$

$$k_s \left(\frac{\partial T_s}{\partial x} \right)_{R^+} = k_f \left(\frac{\partial T_f}{\partial x} \right)_{R^-}$$

$$y = R_i : T_s|_{R^+} = T_f|_{R^-}$$

$$k_s \left(\frac{\partial T_s}{\partial y} \right)_{R^+} = k_f \left(\frac{\partial T_f}{\partial y} \right)_{R^-}$$

Also at the inlet cross-section:

$$y = R_i + h_{ch}; R_i - w_{ch} < x < R; 0 < z < l_{ch} / 2,$$

$$M = M_{in} \text{ and } T = T_{in}$$

All the outer surfaces of the heat sink are insulated except the bottom one in contact with the chip:

$$y = -[H - (D_i + h_{ch}) + R_i]; -W_m < x < W_m;$$

$$0 < z < L / 2,$$

$$q = k_s \frac{\partial T}{\partial y}$$

At the outlet of the microtube the following boundary conditions are prescribed:

$$z = L / 2,$$

$$\frac{\partial v}{\partial z} = 0; \frac{\partial w}{\partial z} = 0; \frac{\partial u}{\partial z} = 0; \frac{\partial T}{\partial z} = 0.$$

Table 1. The geometry, thermal and flow conditions of the micro-tube heat sink

Tablica 1. Geometrija, toplinske i karakteristike strujanja za mikrocijevni izmjenjivač topline

B, cm	$H, \mu m$	L, cm	$b_{ch}, \mu m$	L_{ch}, mm	$h_{ch}, \mu m$
1	1500	1	450	1	150
$w_m, \mu m$	$D_i, \mu m$	N	$M, kg/s$	Re	T_{in}, K
1050	900	10	$7 \cdot 10^{-3}$	5107	293

At the symmetry boundaries:

$$z = 0$$

$$\frac{\partial v}{\partial z} = 0; \frac{\partial w}{\partial z} = 0; \frac{\partial u}{\partial z} = 0; \frac{\partial T}{\partial z} = 0,$$

$$x = \pm W_m / 2$$

$$\frac{\partial v}{\partial x} = 0; \frac{\partial w}{\partial x} = 0; \frac{\partial u}{\partial x} = 0; \frac{\partial T}{\partial x} = 0.$$

The set of the partial differential equations along with the boundary conditions are solved using the Fluent commercial solver [23] with methods described in [24]. The Simple algorithm is used for the velocity-pressure coupling solution and second order upwind scheme for equations discretization. The under-relaxation factors are used for pressure field ($\alpha = 0.3$) and momentum conservation ($\alpha = 0.7$). The convergence criterion is defined as:

$$R^p = \frac{\sum_{cells,p} \left| \sum_{nb} a_{nb} \cdot \phi_{nb} + b - a_p \phi_p \right|}{\sum_{cells,p} |a_p \phi_p|}. \quad (7)$$

3. Results and discussion

The pumping power is defined as:

$$\Pi = M \cdot \frac{\Delta p}{\rho}. \quad (8)$$

The pressure difference is calculated as a difference between the average values at the inlet and outlet cross-sections:

$$\Delta p = p_{in} - p_{out}. \quad (9)$$

Also the Re is defined at the inlet cross-section as:

$$Re = \frac{4 \cdot (M / 2)}{\pi \cdot D \cdot \mu}. \quad (10)$$

In the figure 3 temperature distribution at the bottom sink surface for HFE-7600 and water is presented. Due to compatibility with most electronic components and dielectric strength, HFE-7600 fluid can be used in single and two-phase cooling of supercomputers, sensitive military electronics and also high voltage transformers and power electronics.

Besides, due to the pure thermal properties of the dielectric fluid, even for high pumping power $\Pi = 1.2$ W, the maximum temperature is $T_{max} = 352$ K and temperature difference along the bottom wall is $\Delta T = 7$ K. For the water case and $\Pi = 0.195$ W, $T_{max} = 316$ K and $\Delta T = 1.2$ K.

The temperature distribution for sidewall and bottom wall of the heat sink is presented in the figure 4. The uniform surface temperature is observed except for the portions close to the inlet channel.

The axial velocity distribution is presented in the figure 5. The higher axial velocities are observed at the tube wall surface rather than in the middle of the microtube, that increases the heat transfer coefficient.

Moreover, despite the high heat flux $q = 100 \text{ W/cm}^2$, the single-phase regime is still preserved.

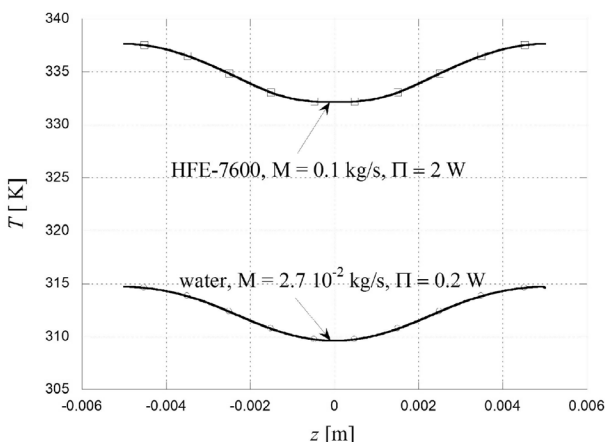


Figure 3. The temperature distribution at the bottom heat sink surface along the fluid flow for HFE 7600 and water

Slika 3. Temperaturna raspodjela na donjoj površini izmjenjivača topline duž strujanja fluida za HFE 7600 i vodu

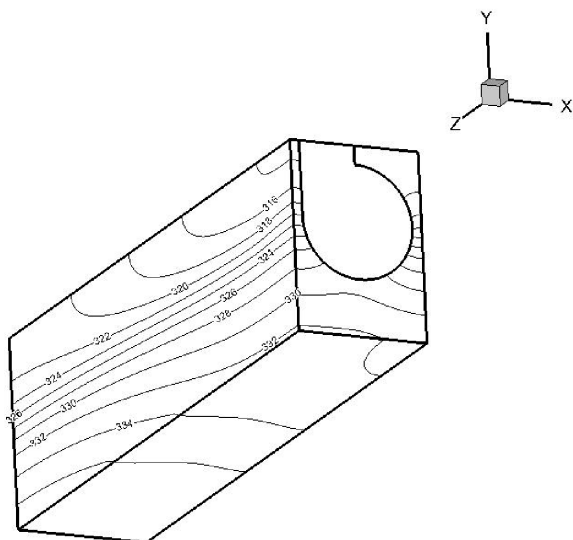


Figure 4. The temperature distribution at the bottom and sidewall heat sink surfaces along the fluid flow for $\Pi = 0.055 \text{ W}$ and two different configurations

Slika 4. Promjena temperature na donjoj površini i poprečnim stijenkama izmjenjivača topline duž strujanja fluida za $\Pi = 0.055 \text{ W}$ i dvije različite konfiguracije

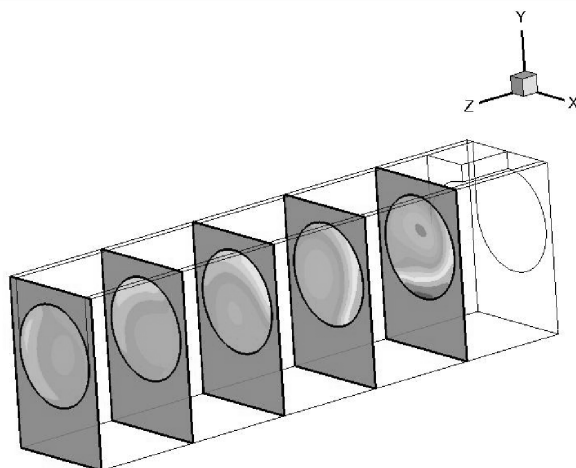


Figure 5. The distribution of axial fluid flow velocity inside the microtube

Slika 5. Raspodjela poprečne brzine strujanja fluida unutar mikrocijevi

Acknowledgements

This work was supported by CNCISIS –UEFISCSU, project number 670 PNII – IDEI 938/2008.

REFERENCES

- [1] TUCKERMAN, DB: *Pease RFW: High-Performance Heat Sinking for VLSI*, IEEE Electron. Device Lett. (1981) EDL-2, 126–129.
- [2] QU, W.; MUDAWAR, I: *Experimental and Numerical Study of Pressure Drop and Heat Transfer in Single-phase Micro-channel Heat Sink*. International Journal of Heat and Mass Transfer 45 (2002) 2549 - 2565.
- [3] FEDOROV, A.; VISKANTA, R: *Three Dimensional Conjugate Heat Transfer in the Microchannel Heat Sink for Electronic Packaging*, International Journal of Heat and Mass Transfer 41 (2000) 399 – 415.
- [4] RAHMAN, M.M.: *Measurements of Heat Transfer in Microchannels Heat Sinks*, International Communications in Heat and Mass Transfer 27 (2000) 495 – 506.
- [5] LI, J.; PETERSON, G.P.; CHENG, P.: *Three-dimensional analysis of heat transfer in a micro-heat sink with single phase flow*, International Journal of Heat and Mass Transfer 47 (2004) 4215 – 4231.
- [6] WEI, X.; JOSHI, Y.K.: *Stacked microchannel heat sinks for liquid cooling of microelectronics component*, ASME Journal of Electronic Packaging 126 (2004) 60–66.

- [7] PATTERSON, M.K.; WEI, X.; JOSHI, Y.; PRASHER, R.: *Numerical study of conjugate heat transfer in stacked microchannel*, Inter Society Conference on Thermal Phenomena (2004) 372-380.
- [8] KIM, S.J.; KIM, D.: *Forced Convection in Microstructures for Electronic Equipment Cooling*. Journal of Heat Transfer 121 (1999) 639-645.
- [9] KIM, S.J.; KIM, D.; LEE, D.Y.: *On the local thermal equilibrium in microchannel heat sink*, International Journal of Heat and Mass Transfer 43 (2000) 1735 - 1748.
- [10] LIU, S.; ZHANG, Y.; LIU, P.: *Heat transfer and pressure drop in fractal microchannel heat sink for cooling of electronic chips*, Heat Mass Transfer 44 (2007) 221-227.
- [11] AYNUR, T.N.; KUDUSSI, L.; EGRICAN, N.: *Viscous dissipation effect on heat transfer characteristics of rectangular microchannels under slip flow regime and H1 boundary conditions*, Heat Mass Transfer 42 (2006) 1093-1101.
- [12] CHEN, C.H.: *Slip-flow heat transfer in a microchannel with viscous dissipation*, Heat Mass Transfer 42 (2006) 853-860.
- [13] HASSAN, I.: *Thermal-Fluid Mems devices: A decade of progress and challenges ahead*, ASME Journal of Heat Transfer 128 (2006) 1221-1233.
- [14] GARIMELLA, S.V.; SOBHAN, C.B.: *Transport in microchannels – a critical review*, Annual Review of Heat Transfer 13 (2003) 1-50.
- [15] KROEKER, C.J.; SOLIMAN, H.M.; ORMISTON, S.J.: *Three-dimensional thermal analysis of heat sinks with circular cooling micro-channels*, International Journal of Heat and Mass Transfer 47 (2004) 4733 - 4744.
- [16] RYU, J.H.; CHOI, D.H.; KIM, S.J.: *Three-dimensional numerical optimization of a manifold microchannel heat sink*, International Journal of Heat and Mass Transfer 46 (2003) 1553 - 1562.
- [17] LELEA, D.: *The heat transfer and fluid flow of a partially heated microchannel heat sink*, International Communications in Heat and Mass Transfer 36(8) (2009) 794-798.
- [18] LELEA, D.: *The performance evaluation of Al_2O_3 /water nanofluid flow and heat transfer in microchannel heat sink*, International Journal of Heat and Mass Transfer, Article in press (2011), doi: 10.1016/j.ijheatmasstransfer.2011.04.038
- [19] SUNG, M.K.; MUDAWAR, I.: *Experimental and numerical investigation of single-phase heat transfer using a hybrid jet-impingement/micro-channel cooling scheme*, International Journal of Heat and Mass Transfer 49 (2006) 682 - 694.
- [20] LELEA, D.: *The microtube heat sink with tangential impingement jet and variable fluid properties*, Heat and Mass Transfer 45(9) (2009) 1215 - 1222
- [21] LELEA, D.: *Effects of inlet geometry on heat transfer and fluid flow of tangential micro-heat sink*, International Journal of Heat and Mass Transfer 53 (2010) 3562-3569.
- [22] 3M™ Novec™ 7600 Engineered Fluid, 3M Electronics Markets Materials Division.
- [23] Fluent 6.1.22 documentation. Fluent Inc. 2003.
- [24] PATANKAR, S.V.: *Numerical Heat Transfer and Fluid Flow*, McGraw Hill, (1980).